

Generation of Pulsed Fe Plasma and Study of Its Physical Parameters

Naseer M. Hadi¹, Sabah H. Sabeeh² and Mustafa M. R. Sabhan³

Laser & Electro-Optics Research Center, Ministry of Science and Technology, Baghdad, Iraq¹

Department of Applied Science, University of Technology, Baghdad, Iraq²

P.G. Student, Department of Applied Science, University of Technology, Baghdad, Iraq³

ABSTRACT: In the present work, a pulsed Fe plasma generation by Q-switched Nd: YAG laser. The energy per pulse at the target surface was fixed at a level of (475 mJ, 6 ns), focused on Fe solid target at atmospheric pressure and vacuum pressure (1×10^{-1} mbar). The plasma temperature was measured from Boltzmann plot using six Fe I spectral lines at the wavelengths (501.2, 534.1, 556.9, 576.2, 602.4 and 623.07) nm. The electron density was measured by means of Stark broadening formula (FWHM) for spectral lines Fe I at line transition 576.2 nm and for Fe I at line transition 556.9 nm as the reference electron density, at atmospheric pressure and vacuum pressure. The density was $8.2 \times 10^{18} \text{ cm}^{-3}$ and electron temperature 1.466 eV at atmospheric pressure, the electron density was $9 \times 10^{18} \text{ cm}^{-3}$ and the electron temperature 1.711 eV at pressure (1×10^{-1}) mbar. Measurements were done based on theory of local thermodynamic equilibrium (LTE) in the range (500-650 nm) of emitted spectrum.

KEYWORDS: Laser-produced plasma; Plasma parameters; Fe plasma; Temperature; Electron density.

I. INTRODUCTION

Laser-produced plasma spectroscopy (LPPS) also called Laser Induced Plasma spectroscopy (LIPS) is one of the most fruitful methods using solid, liquid and gas target. LPPS uses a low-energy pulsed laser (typically tens to hundreds of mill joules per pulse) to generate a plasma which vaporizes a small amount of the sample [1]. The invention of the laser produced plasma in the mid-1970s led to increase in knowledge on interaction between electromagnetic fields and matter. Laser-produced plasmas applied to various areas in different fields of science. Laser produced plasma is better than an electric discharge because of the high efficiency, cleanliness and large collection angle [2]. Plasmas and laser-produced plasma applications classified as [3-6]. Plasma processing such as plasma surface cleaning, plasma thin film deposition, plasma hardening and plasma in medicine such as surface treatment, sterilization of medical instruments. Laser produced plasma has high temperature and high electron density gradient, this plasma is also high irradiative, it's emitted a spectrum deepening on the target, the emitted spectrum gives information about the target. Spectroscopic method is one of plasma diagnostic, which can used it to measure the electron temperature and electron density from the emitted spectrum [7].

Temperature is one of the most important parameters used to characterize the state of the plasma. Most important spectroscopic techniques, for electron temperature, are the ratio of lines produced in sequential charge states of a single species. An accurate knowledge of the temperature leads to an understanding of the occurring plasma processes, namely vaporization, dissociation, excitation, ionization and transition probability. Plasma electron temperature can be measured from the relative intensity of two or more optically thin lines having small separation in the emission wavelength and large separation in their upper excited states (Boltzmann plot method) [8]. Moreover, the ionization temperature can be calculated from the relative intensity of two or more lines originating from two consecutive ionization stages. This method enhances the precision in measuring temperature due to enhancement of the separation of the upper excited states by the ionization energy (Saha-Boltzmann plot) [9].

On the other hand, the electron density can be measured using the Stark broadening formula of optically thin emitted spectral lines from neutral atoms or ions with the help of the precise Stark broadening parameters that can be found in different standard Tables [10,11].

International Journal of Innovative Research in Science, Engineering and Technology

(An ISO 3297: 2007 Certified Organization)

Vol. 4, Issue 1, January 2015

In this paper, we will describe the experiment, used to produce plasma from solid Fe target. The emission spectrum detected and analysis the intensity of it to diagnostic the electron temperature and electron density. The measurements of temperature based on relative line intensities of two lines given by equation [12]:

$$\ln \left(\frac{I_Z \lambda_{ki,Z}}{g_{k,Z} A_{ki,Z}} \right) = - \frac{1}{k_B T} E_{k,Z} + \ln \left(\frac{hc L n_Z}{4\pi P_Z} \right) \dots\dots\dots (1)$$

where the Z refers to the ionization stage. k_B is the Boltzmann constant, T is the plasma temperature. $E_{k,Z}$ and $g_{k,Z}$ are energy and degeneracy of the upper energy level k respectively. n_Z is the density number, and P_Z is the partition function of the species in ionization stage Z. L is the characteristic length of the plasma, $A_{ki,Z}$ is the transition probability I_Z is The integrated intensity of a spectral line occurring between the upper energy level k and the lower energy level i of the species in ionization stage Z in optically thin plasma. This yields a linear plot (Boltzmann plot) if one represents the magnitude on the left-hand side for several transitions against the energy of the upper level of the species in ionization stage Z. The value of T was deduced from the slope of the Boltzmann plot.

Electron density can be determined from the line broadening of Stark broadening formula. Laser produced plasma the most broadening is Stark broadening, this broadening results from collisions by electrons and ions. The optical emission spectroscopy (OES) is the tool by which the plasma can be diagnosed [13]. The diagnostics of the plasma can be done through the measurements of electron density (N_e) and temperature (T_e). By measurements of the Stark broadened from line profile of an isolated atom or singly charged ion and calculate the full width at half maximum (FWHM) of the line, $\Delta\lambda_{1/2}$, which is related to the electron density (N_e) by the expression equation [14]:

$$\Delta\lambda_{\frac{1}{2}} = 2w \left(\frac{N_e}{10^{16}} \right) \quad \text{in } \text{\AA} \quad \dots\dots\dots (2)$$

where w is the electron impact width parameter or Stark width parameter, N_e is electron density number. The Stark width parameter (w) of these lines and atomic data of the selected spectra lines are taken from reference [15, 16]. The measured widths (FWHM) agree fairly well with semi-classical calculations. They are usually normalized to a reference electron density $N_r=10^{16} \text{ cm}^{-3}$.

II. EXPERIMENTAL SETUP

A Q-switched Nd: YAG laser model (RY580) was used at the fundamental wavelength (1064 nm). Repetition rate of (1Hz) is use for laser-produced plasma. The output pulse duration is (6 ns) and the maximum pulse energy (500 mJ), which is measure by a Gentec-EO MAESTRO joule meter. A schematic diagram of experimental set-up and the vacuum chamber is shown in Figure (1). The target holder was fixed at 45° direction in order to ensure that the plasma emission is right-angled with respect to the diagnostic tools. The distance between the target and the laser is 10 cm. The laser is focus on the target by a quartz lens of focal length of 5 cm, the vacuum chamber was evacuated using a rotary pump. Silicon Photo Detector (model DSi 200) was used to detect the visible and UV photons which were produced by laser produced plasma, wavelength in the range of 200-1100 (nm). Pure commercial metal target of Fe was used as target in the present work. A computerized Omni-Lambda 150 grating monochromator device was used.

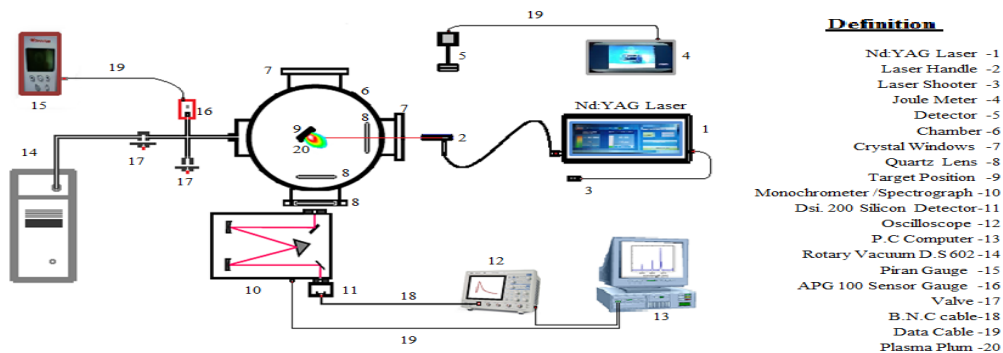


Figure (1): A Schematic Diagram of Experimental Set-Up.

III. RESULTS AND DISCUSSIONS

Results of the present work include the measurement of electron temperature assuming the local thermodynamic equilibrium (LTE) and electron density determine by using Stark broadening in optically thin plasma conditions. The present work include the study of the effect of the surrounding pressure on the plasma intensity at wavelength region [500-650 nm] has done also. All data points were fitted with Lorentzian fitting function using Curve Expert Professional software version 2.0.3.

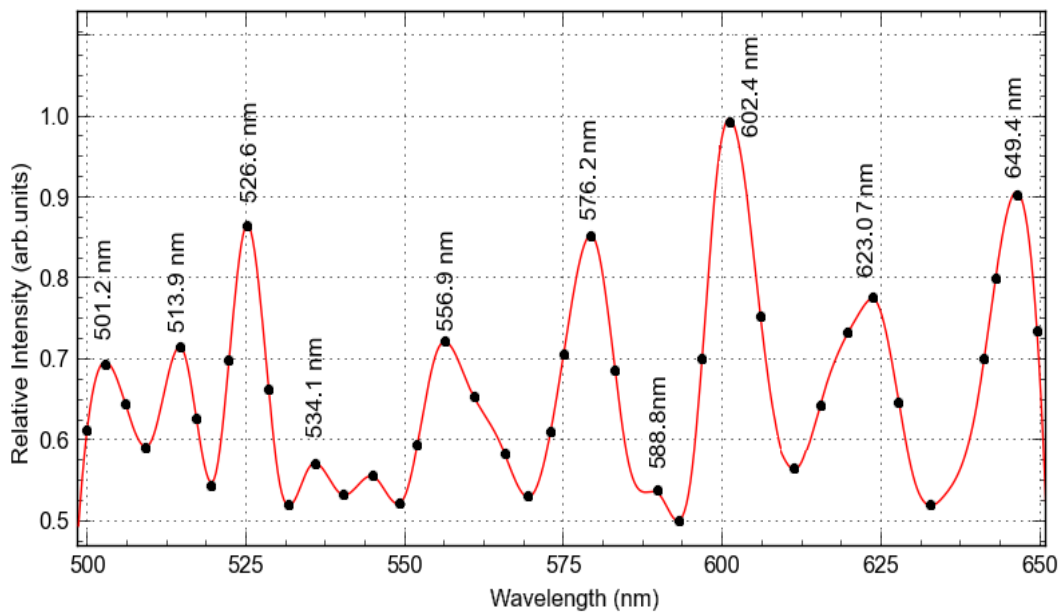


Figure (2): The emission spectrum of the produced Fe plasma at atmospheric pressure in spectral range [500-650 nm] for laser energies 475 mJ and power density ($1 \times 10^{12} \text{ W cm}^{-2}$) at zero delay time. The relative error of the fitting line is 4%.

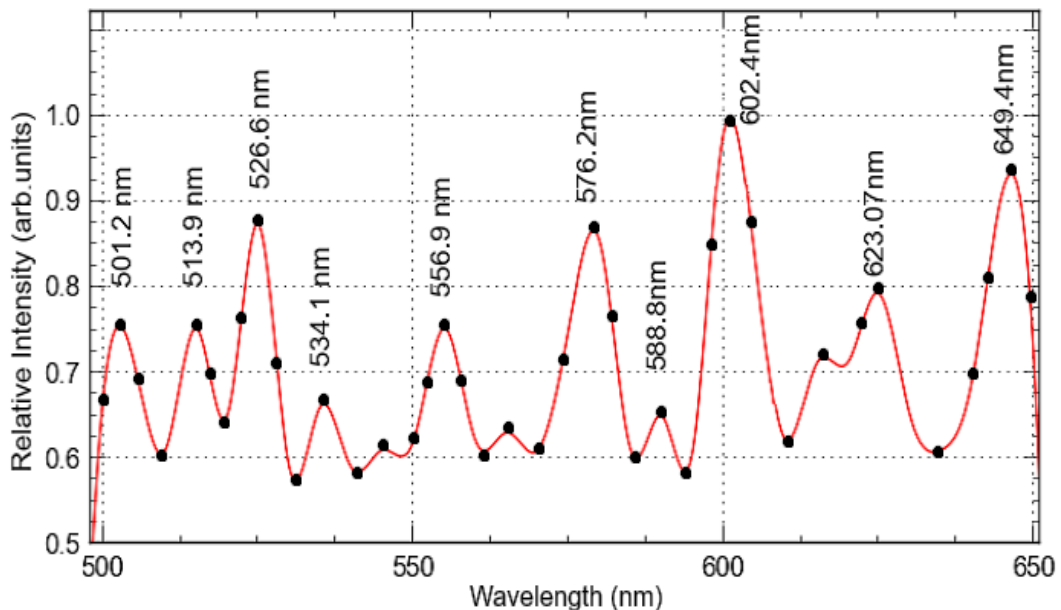


Figure (3): The emission spectrum of the produced Fe plasma at vacuum pressure reaching (1×10^{-1} mbar) in spectral range [500-650 nm] for laser energies 475 mJ and power density ($1 \times 10^{12} \text{ W cm}^{-2}$) at zero delay time. The relative error of the fitting line is 4%.

International Journal of Innovative Research in Science, Engineering and Technology

(An ISO 3297: 2007 Certified Organization)

Vol. 4, Issue 1, January 2015

Table (1): Spectral lines of Fe I and their atomic data [10,11,15].

| Wavelength (nm) | Spectrum | A_{ki} (s^{-1}) | E_i (cm^{-1}) | E_k (cm^{-1}) | g_i | g_k |
|-----------------|----------|-----------------------|---------------------|---------------------|-------|-------|
| 501.206 | Fe I | 5.50E+04 | 6 928.268 | 26 874.550 | 11 | 11 |
| 513.925 | Fe I | 9.16E+06 | 24 180.862 | 43 633.533 | 7 | 5 |
| 526.655 | Fe I | 1.10E+07 | 24 180.862 | 43 163.326 | 7 | 9 |
| 534.102 | Fe I | 5.21E+05 | 12 968.554 | 31 686.351 | 5 | 5 |
| 556.961 | Fe I | 2.34E+07 | 27 559.583 | 45 509.152 | 5 | 3 |
| 576.299 | Fe I | 9.60E+06 | 33 946.933 | 51 294.220 | 5 | 7 |
| 588.881 | Fe I | 1.9E+06 | 37 409.555 | 54 386.186 | 3 | 3 |
| 602.405 | Fe I | 1.69E+04 | 36 686.176 | 53 281.689 | 9 | 11 |
| 623.072 | Fe I | 9.99E+05 | 20 641.110 | 36 686.176 | 9 | 9 |
| 649.498 | Fe I | 7.66E+05 | 19 390.168 | 34 782.421 | 13 | 11 |

The plasma temperature measurement for Fe plasma is developed from Boltzmann plot using six Fe I spectral lines at the wavelengths (501.2, 534.1, 556.9, 576.2, 602.4 and 623.07) nm at laser energies 475 mJ. Using equation (1) and plotting $\ln(I\lambda / gA_{ki})$ versus E_{exc} should yields a straight line with a slope equal to $(-1/kT)$. The parameters of Fe I spectral lines get it from Reference [10,11,15,16]. However, these lines would be good candidates for calculating the plasma electron temperature. The wavelength separation is very small as well as their separation in the upper excited states is relatively large with the expected plasma temperature (~ 1 eV) [13].

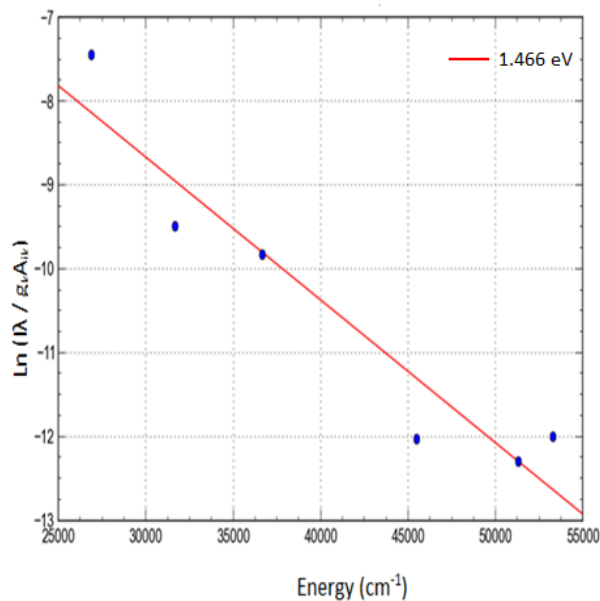


Figure (4): Boltzmann plot for laser produced Fe plasma at atmospheric pressure equal to $(1 \times 10^{-3}$ mbar). The relative error of the slope is 0.86% and the plasma temperature is $T = 1.466$ eV (16997.1 K).

International Journal of Innovative Research in Science, Engineering and Technology

(An ISO 3297: 2007 Certified Organization)

Vol. 4, Issue 1, January 2015

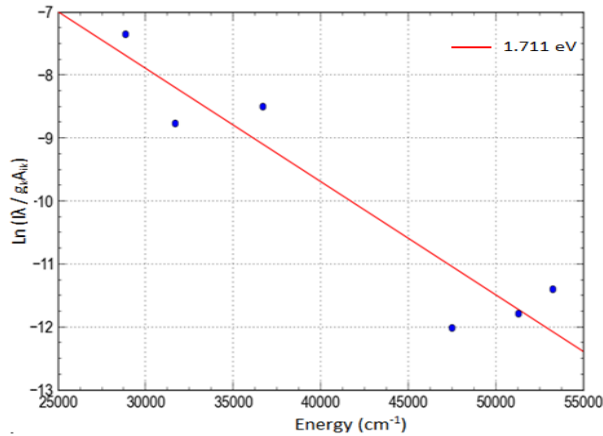


Figure (5): Boltzmann plot for laser-produced Fe plasma at vacuum pressure equal to (1×10^{-1} mbar). The relative error of the slop is 0.74% and the plasma temperature is $T= 1.711\text{eV}$ (19837.6 K).

Fig. (4) shows that the temperature is 1.466 eV at atmospheric pressure. Fig. (5) shows that the temperature is 1.711 eV at pressure 1×10^{-1} mbar, the deference in electron temperature due to difference of pressure, due to the presence of O_2 molecules. The O_2 molecules are electronegative ions. This gas can react strongly with plasma electrons and reduce the mean free path.

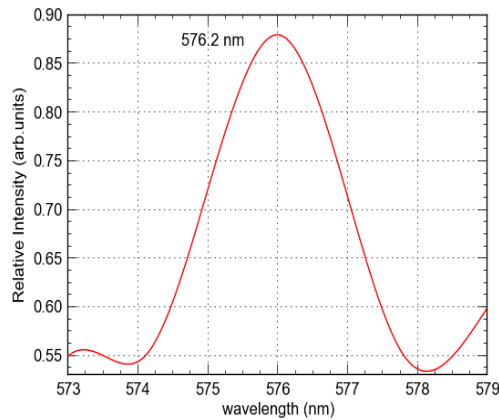


Figure (6): Spectral profile of Fe I at 576.2 nm at atmospheric pressure ($1 \times 10^{+3}$ mbar, power density 1×10^{12} W/ cm^2) at zero delay time. The relative error of the fitting line is 1%.

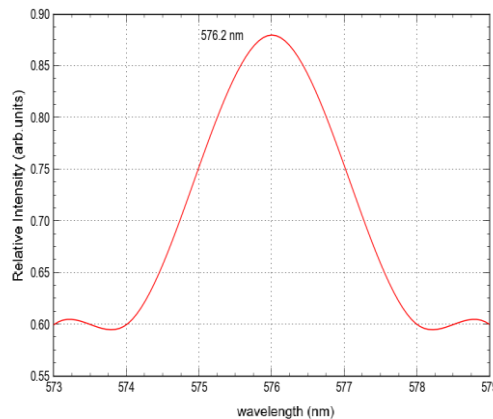


Figure (7): Spectral profile of Fe I at 576.2 nm at vacuum pressure (1×10^{-1} mbar, power density 1×10^{12} W/ cm^2).The relative error of the fitting line is 1.1%.

International Journal of Innovative Research in Science, Engineering and Technology

(An ISO 3297: 2007 Certified Organization)

Vol. 4, Issue 1, January 2015

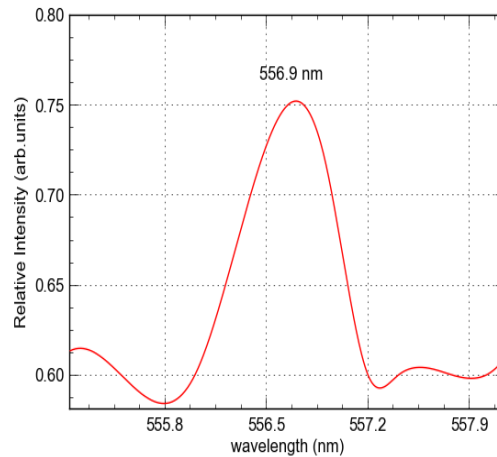


Figure (8): Spectral profile of Fe I at 556.9 nm at vacuum pressure (1×10^{-1} mbar, power density 1×10^{12} W/cm²). The relative error of the fitting line is 1%.

Plasma generated by laser characterized by high density, so Stark effect is leads to a broadening of emitted lines. By using equation (2) we determine the electron density of spectral lines Fe I at line transition 576.2 nm at atmospheric pressure as shown in Fig. (6) and Fe I at 576.2 nm at pressure 10^{-1} mbar as shown in Fig. (7). The electron density is (8.2×10^{18} cm⁻³) at atmospheric pressure and at pressure 10^{-1} mbar the electron density is (9×10^{18} cm⁻³). Also the electron density measured for spectral lines Fe I at line transition 556.9 nm at pressure 10^{-1} mbar as shown in Fig. (8), the electron density is (9.2×10^{18} cm⁻³). Effect of O₂ on the temperature can be seen also on the electron density. Results of the present work shows, the higher temperatures and electron densities are obtained in vacuum pressure (1×10^{-1} mbar), and the lower ones are found in atmospheric pressure. The presence of this line was attributed to the existence of a very small concentration of water vapour (humidity) around the target [17].

IV. CONCLUSION

We have measured the plasma electron temperature using six spectral lines for electron temperature measurement and two lines for electron density measurement emerging from iron in LPP experiment. Temperature was calculated from line intensity ratios of successive ionization stages of iron and using six Fe I spectral lines for measured the plasma electron temperature in order to get more accuracy in measurement. The density was determined from the Stark broadening of iron lines from its first ionization stage, and results from both lines were identical within experimental error. Also compare the results generated under the two types of environment air, a first under atmospheric pressure and secondly under vacuum pressure. Results showed a higher temperature value and density at vacuum pressure compared to the results that appeared at atmospheric pressure. Because of oxygen molecules that constantly surround the plasma, where it leads to reduce the mean free path between molecules and leads to reduce the number of collisions between plasma molecules. Plasma expands rapidly, but this expansion is slowed down and finally stopped by the resistance of oxygen molecules around the target. The electron density were re-evaluated and compared to reference density utilizing the Fe I at line transition 556.9 nm. This comparison shows an excellent agreement between the reference density and the measured utilizing the iron emission lines.

REFERENCES

1. D. A. Cremers and L. J. Radziemski, "Handbook of Laser-Induced Breakdown Spectroscopy", John Wiley & Sons Ltd, West Sussex, 2006.
2. P. T. Rumsby, J. W. M. Paul, and M. M. Masoud, "Control Fusion", Plasma Phys. Vol. 16, No. 969, 1974.
3. A. Bers and A. K. Ram, "Plasma Electrodynamics and Applications", RLE Progress Report 144, 2002.
4. U. Teubner and P. Gibbon, Rev. Modern Phys., Vol. 81, No. 445, 2009.
5. Ph. Nicolai, V. T. Tikhonchuk, A. Kasperczuk, T. Pisarczyk, S. Borodziuk, K. Rohlena, and J. Ullschmied, Physics Plasma, Vol. 13, No. 062701, 2006.
6. Y. Tao, M. S. Tillack, K. L. Sequoia, R. A. Burdt, S. Yuspeh, and F. Najmabadi, Applied Physics Letter, Vol. 92, No. 251501, 2008.
7. J. H. Donne, "Introduction to the Plasma Diagnostics", Journal of Fusion Science and Technology, Vol. 53, pp. 379-386, 2008.

International Journal of Innovative Research in Science, Engineering and Technology

(An ISO 3297: 2007 Certified Organization)

Vol. 4, Issue 1, January 2015

8. De Giacomo, M. Dell'Aglio, F. Colao and R. Fantoni, "Double Pulse Laser Produced Plasma on Metallic Target in Seawater Basic Aspects and Analytical Approach", *Spectrochim Acta Part B*, Vol. 59, No. 9, pp. 1431- 1438, 2004.
9. W. Lochte-Holtgreven, "Plasma Diagnostics", North Holland, Amsterdam, 1968.
10. NIST Atomic Energy Levels Data Center, NIST Data Base For Atomic Spectroscopy, National Institute of Standards and Technology, USA, 1995.
11. J. E. Sansonetti and W. C. Martin," Hand Book of Basic Atomic Spectroscopic Data", National Institute of Standards and Technology, American Institute of Physics, Gaithersburg, Maryland, 2005.
12. V. K. Unnikrishnan, Kamlesh Alti, V. B. Kartha, C. Santhosh, G. P. Gupta, and B. M. Suri, "Measurements of Plasma Temperature and Electron Density in Laser-Induced Copper Plasma by Time-Resolved Spectroscopy of Neutral Atom and Ion Emissions", *Pramana, Journal of Physics*, Vol. 74, No. 6, pp. 983-993, 2010.
13. H. R. Griem, "Plasma Spectroscopy", McGraw-Hill, Boston, 1964.
14. R. K. Singh, O. W. Holland and J. Narayan, "Theoretical Model for Deposition of Superconducting Thin Films Using Pulsed Laser Evaporation Technique", *Journal of Applied Physics*, Vol. 68, No. 1, pp. 233-147, 1990.
15. W. Allen, M. Blaha, W. W. Jones, A. Sanchez, and H. R. Griem, *Phys. Rev. A*, Vol. 11, No. 477, 1975.
16. H. R. Griem, "Plasma Spectroscopy", McGraw-Hill Book Company, New York, 1964.
17. M. El Sherbini, Th. M. El Sherbini, H. Hegazy, G. Cristoforetti, S. Legnaioli, V. Palleschi, L. Pardini, A. Salvetti and E. Tognoni, "Evaluation of Self-Absorption Coefficients of Aluminum Emission Lines in Laser-Induced Breakdown Spectroscopy Measurements", *Spectrochimica Acta Part B*, Vol. 60, No. 12, 2005.